Research Square

Preprints are preliminary reports that have not undergone peer review. They should not be considered conclusive, used to inform clinical practice, or referenced by the media as validated information.

The initial condition as a decaying forcing: ageing and Lyapunov exponents of fractional maps

Stefano Fazzino

sfazzino@gmail.com

University of Catania https://orcid.org/0000-0002-3015-4938

Research Article

Keywords: fractional difference maps, fractional logistic map, Lyapunov exponents, diffusive representation, power-law memory, ageing

Posted Date: October 22nd, 2026

DOI: https://doi.org/10.21203/rs.3.rs-11456319/v1

License: This work is licensed under a Creative Commons Attribution 4.0 International License. Read Full License

Additional Declarations: The authors declare no competing interests.

Highlights

The initial condition as a decaying forcing: ageing and Lyapunov exponents of fractional maps

Stefano Fazzino

- Caputo fractional maps are autonomous maps on a space of memory modes
- A hundred to two hundred modes reproduce the memory kernels over 10^8 steps
- The initial condition acts as a forcing decaying as $(x_0 - \bar{x})\, n^{-\nu}$
- Along regular orbits the sensitivity decays as $n^{-\nu}$ and the exponents are zero
- Chaotic statistics age, but not along orbits started at the time average

The initial condition as a decaying forcing: ageing and Lyapunov exponents of fractional maps

Stefano Fazzino

Independent researcher, Catania, Italy

Abstract

Fractional difference maps are recurrences in which the new state depends on the whole past orbit through weights that decay as a power of the elapsed time, and a consistent quantitative description of their chaotic regimes is still missing. We show that the fractional logistic maps of Caputo type, both with the falling-factorial kernel and with the power-law kernel, can be rewritten exactly as autonomous maps on a space of memory modes. The rewriting rests on the fact that the two kernels are moment sequences of positive measures on the unit interval, in the first case of a Beta distribution. A trapezoidal quadrature in a logarithmic variable reproduces the kernels with a relative error below $4 \cdot 10^{-7}$ over 10^8 steps with 100 to 200 modes, so that the cost of an orbit grows linearly, and not quadratically, with its length, and the Lyapunov exponents can be defined on the space of modes without any truncation of memory. We then show that the Caputo initial condition x_0 is equivalent to a past history frozen at x_0, which acts on the dynamics as a forcing proportional to $(x_0 - \bar{x})\, n^{-\nu}$, where n is the number of iterations, $\bar{x}$ the time average of the orbit and ν the fractional order. In the numerical experiments, along orbits attracted by fixed points or periodic sinks the derivative of the state with respect to x_0 decays as $n^{-\nu}$, so that the exponents are zero. In the chaotic regime the local expansion rate keeps a memory of the initial condition which, at $\nu = 0.3$ and 0.35, is still visible after 10^7 iterations; at large n it decays as a power of n with an exponent close to ν, and its amplitude grows with $|x_0 - \bar{x}|$. Orbits started close to $\bar{x}$ do not show this drift. The same behaviour is found in a fractional Hénon map.

Email addresses: `sfazzino@gmail.com` (Stefano Fazzino), `sfazzino@dieei.unict.it` (Stefano Fazzino)

Keywords: fractional difference maps, fractional logistic map, Lyapunov exponents, diffusive representation, power-law memory, ageing

1. Introduction

Discrete maps with memory are the simplest systems in which we can study how a long memory changes a nonlinear dynamics. Among them, fractional difference maps have attracted increasing attention in the last ten years. In these maps the new state is computed from the whole past orbit through a weighted sum, and the weight given to a past state decays as a power of the time elapsed since then; in mathematical terms, the map is a Volterra recurrence of convolution type. Such maps arise from the discretization of fractional differential equations [1, 2] and, independently, from the discrete fractional calculus, where difference operators of Riemann–Liouville and Caputo type are defined directly on the integers [3, 4]. The best known examples are the fractional logistic map introduced by Wu and Baleanu [5] and the family of fractional maps studied systematically by Edelman [6, 7, 8]. These maps do not behave like their integer-order counterparts. Their orbits approach fixed points and periodic sinks only as a power of time, a cascade of bifurcations may take place along a single trajectory, and the bifurcation diagrams change with the initial condition and with the number of iterations [6, 8].

Much less is known about their chaotic regimes. Lyapunov exponents are usually computed with the Jacobian algorithm that Wu and Baleanu extended to maps with memory [10], in which the tangent map is obtained by differentiating the whole Volterra sum. This procedure does not say on which space the exponents are defined, and it is not known whether its finite-time estimates converge. Edelman observed that for a map of Caputo type converging to a fixed point a correctly computed exponent should be zero, because the convergence is algebraic, whereas negative values have been reported [7]; in his recent review he lists a consistent quantitative analysis of chaos in discrete fractional systems among the open problems of the field [8]. There is also a practical obstacle. Since every step involves the whole past, an orbit of length N costs a time proportional to N^2, and the transients of these maps, which at small orders may last 10^5 or 10^6 iterations [6], are expensive to follow.

The situation is similar for fractional-order differential systems, whose exponents have been computed for many years [11, 12] without a definition

of the object being computed. In a previous work [14] we proposed to define them through the diffusive representation of the fractional integral [15], which turns the system into an autonomous evolution equation on a space of memory modes. We also showed that the memory of a Caputo trajectory ages, i.e., that it keeps growing for the whole life of the system, and we conjectured that, as a consequence, the finite-time exponents converge with an algebraic correction proportional to $t^{-\nu}$, where ν is the order. This correction is hidden by the statistical fluctuations of time averages, which decay as $t^{-1/2}$, unless $\nu < 1/2$, and the fractional oscillators used as benchmarks are not chaotic at such low orders. Discrete fractional maps, on the contrary, are chaotic at small orders [6], and they are therefore the natural place where the ageing of a chaotic dynamics can be observed.

In this paper we carry the construction over to discrete time. We first show that the two kernels of the fractional logistic maps of Caputo type are moment sequences of positive measures on the unit interval. This allows us to rewrite the maps exactly as autonomous maps whose state is a function on that interval: each value of the function is a memory mode, which forgets geometrically and is fed by the current state. A trapezoidal quadrature in a logarithmic variable gives a finite-dimensional version of the map whose cost grows linearly with the length of the orbit, so that a hundred orbits of 10^8 steps can be followed on a laptop computer. On the space of modes the tangent map is a multiplication operator plus an operator of rank one, and the Lyapunov exponents can be defined and computed without truncating the memory. We then rewrite the map in terms of the deviations of the orbit from a constant ξ and find a forcing proportional to $x_0 - \xi$ that decays as $n^{-\nu}$, where x_0 is the initial condition and n the number of iterations. When ξ is the time average $\bar{x}$ of the orbit, this forcing is the leading effect of the initial condition, and it explains two facts that we observe in the simulations. Along orbits attracted by fixed points or periodic sinks, the derivative of the state with respect to x_0 decays as $n^{-\nu}$, so that the exponents are zero and negative values can only come from finite horizons. In the chaotic regime the local expansion rate depends on the initial condition for a time much longer than the correlation time of the dynamics, and at large n this dependence decays as a power of n with an exponent close to ν. Orbits started close to the time average do not show this dependence, which suggests a simple rule for the computation of exponents of fractional maps. We have checked that none of this depends on the logistic nonlinearity by repeating the analysis on a fractional Hénon map.

The paper is organized as follows. In Section 2 we introduce the maps, their representation on memory modes, the tangent map and the quadrature. In Section 3 we show how the initial condition enters the dynamics. Section 4 contains the numerical results: accuracy and cost of the method, bifurcations and exponents at low orders, the ageing of chaotic statistics in the FDLM and in the Hénon map. Sections 5 and 6 contain the discussion and the conclusions, and the Appendix the proof of the result of Section 3.

2. Fractional logistic maps and their memory modes

2.1. The maps

Let $0 < \nu < 1$ be the fractional order and $K > 0$ a parameter. Following Edelman [8], we write the fractional logistic maps of Caputo type as

$$x_{n+1} = x_0 - \sum_{k=0}^{n} c(n-k)\, G_K(x_k), \qquad G_K(x) = x - Kx(1-x), \qquad n \geq 0. \quad (1)$$

Here x_0 is the initial condition, which appears explicitly in the map, as in the Caputo derivative, and $c(m)$ is the weight given to the state x_k when $m = n - k$ steps have elapsed since then. We call m the lag. The kernel c is one of the two sequences

$$c_{\mathrm{D}}(m) = \frac{\Gamma(m+\nu)}{\Gamma(\nu)\,\Gamma(m+1)}, \qquad c_{\mathrm{P}}(m) = \frac{(m+1)^{\nu-1}}{\Gamma(\nu)}, \qquad m = 0, 1, 2, \ldots, \quad (2)$$

where Γ is the Euler gamma function. The kernel c_{D} comes from the falling factorial $t^{(\nu)} = \Gamma(t+1)/\Gamma(t+1-\nu)$ on which the fractional differences of the discrete fractional calculus are built [3, 4], and with this kernel Eq. (1) is the fractional difference logistic map, which we call FDLM. The kernel c_{P} is the kernel $t^{\nu-1}/\Gamma(\nu)$ of the Riemann–Liouville integral sampled at integer times, and with it Eq. (1) is the map that Edelman calls the fractional logistic map, FLM [8]. The subscripts recall the two origins, differences and powers. When we speak of fractional logistic maps without further specification we mean both of them.

For $\nu = 1$ both kernels are equal to one, and subtracting two consecutive equations (1) we find $x_{n+1} = x_n - G_K(x_n) = Kx_n(1 - x_n)$, the ordinary logistic map. For $\nu < 1$ both kernels decay as $m^{\nu-1}/\Gamma(\nu)$, their partial sums grow as $n^{\nu}/\Gamma(\nu+1)$, and every past state keeps contributing to the new one with a weight that decreases slowly with the lag. The integer n, i.e., the number of iterations since the initial condition, will be called the age of the orbit.

2.2. Representation on memory modes

The two kernels have a property that is not apparent from Eq. (2): they are moment sequences of positive measures on the interval $[0, 1]$. For c_{D} the measure is the Beta distribution with parameters ν and $1-\nu$, whose moments are $\Gamma(\nu+m)\Gamma(1)/[\Gamma(\nu)\Gamma(1+m)] = c_{\mathrm{D}}(m)$. For c_{P} we write the power as an integral of exponentials,

$$(m+1)^{\nu-1} = \frac{1}{\Gamma(1-\nu)} \int_0^\infty s^{-\nu} e^{-s(m+1)}\, ds,$$

use the reflection formula $\Gamma(\nu)\Gamma(1-\nu) = \pi/\sin \pi\nu$ and change variable to $r = e^{-s}$. In both cases we obtain

$$c(m) = \int_0^1 r^m \, d\beta(r), \tag{3}$$

with the measures

$$d\beta_{\mathrm{D}}(r) = \frac{\sin \pi\nu}{\pi}\, r^{\nu-1}(1-r)^{-\nu}\, dr, \qquad d\beta_{\mathrm{P}}(r) = \frac{\sin \pi\nu}{\pi}\, (-\ln r)^{-\nu}\, dr. \tag{4}$$

The measure β_{D} has total mass one, while β_{P} has total mass $c_{\mathrm{P}}(0) = 1/\Gamma(\nu)$. According to the moment theorem of Hausdorff, a sequence can be written as in Eq. (3) if and only if it is completely monotone, i.e., if its successive forward differences alternate in sign [16]. The two kernels are therefore completely monotone, a property that Ferreira has recently used for related kernels in the study of linear Volterra difference equations [17].

Equation (3) says that the weight of a past state is an average of geometric sequences r^m, and this suggests following each of them separately. Inserting Eq. (3) into Eq. (1) and exchanging sum and integral, we obtain

$$x_{n+1} = x_0 - \int_0^1 z_n(r)\, d\beta(r), \qquad z_n(r) = \sum_{k=0}^{n} r^{\,n-k}\, G_K(x_k). \tag{5}$$

We call the function $z_n(r)$ the memory of the orbit at age n, and its value at a given r the memory mode with decay factor r. Each mode is a sum of the past values of G_K weighted geometrically, so that it remembers the past for a short time when r is close to zero and for a long time when r is close to one. In the same way as the diffusive representation writes the kernel $t^{\nu-1}/\Gamma(\nu)$ of the Riemann–Liouville integral as a superposition of exponentials $e^{-\omega t}$ [15, 14], Eq. (3) writes the discrete kernel as a superposition of geometric

sequences; the rate ω of the continuous case corresponds here to $s = -\ln r$, which we call the rate of the mode. The advantage of Eq. (5) is that the modes are updated locally in time, since $z_n(r) = r\, z_{n-1}(r) + G_K(x_n)$. Calling η the constant x_0, which never changes, we can therefore write the map as an autonomous map on the pair (η, z):

$$\eta_{n+1} = \eta_n, \qquad z_n(r) = r\, z_{n-1}(r) + G_K\Big(\eta_n - \int_0^1 z_{n-1}\, d\beta\Big), \tag{6}$$

with $\eta_0 = x_0$ and $z_{-1} = 0$. The state at age n is the pair (η_n, z_{n-1}), from which the value of the orbit, which we call the observable, is read as

$$x_n = \eta_n - \int_0^1 z_{n-1}\, d\beta. \tag{7}$$

A convenient state space is $X = \mathbb{R} \times L^2(\beta)$, the product of the real line with the space of functions of r that are square integrable with respect to β, with the norm $\|(\eta, z)\|^2 = \eta^2 + \int_0^1 z^2\, d\beta$. Since β has finite mass, the constant functions belong to $L^2(\beta)$ and the functional $z \mapsto \int z\, d\beta$ is bounded, so that the map (6) is well defined on X. We can collect what we have found in the following statement.

Proposition 1. *For both kernels* (2) *and the corresponding measures* (4)*, the orbit of the map* (1) *starting from* x_0 *coincides with the observable* (7) *of the orbit of the autonomous map* (6) *on* X *starting from the state* $(x_0, 0)$*.*

2.3. Tangent map and Lyapunov exponents

Let $v_n = (\delta\eta_n, \delta z_{n-1})$ be a tangent vector at the state of age n, and let $\delta x_n = \delta\eta_n - \int_0^1 \delta z_{n-1}\, d\beta$ be the corresponding perturbation of the observable. Differentiating Eq. (6) we obtain

$$\delta\eta_{n+1} = \delta\eta_n, \qquad \delta z_n(r) = r\, \delta z_{n-1}(r) + G'_K(x_n)\, \delta x_n, \tag{8}$$

where $G'_K(x) = 1 - K(1 - 2x)$. The operator that maps the memory perturbation δz_{n-1} into δz_n is therefore the multiplication by r plus an operator of rank one. The multiplication by r is a contraction of norm one on $L^2(\beta)$, and its spectrum is the support of β, i.e., the whole interval $[0, 1]$: the slow modes, with r close to one, are contracted by factors arbitrarily close to one. The product of n tangent operators differs from the multiplication by r^n by an operator of finite rank, which is compact, and its measure of non-compactness,

i.e., the distance of the operator from the set of compact operators, is therefore one. In the language of the multiplicative ergodic theorem for products of operators along an orbit [18, 19], the growth rate of this measure, called the essential exponent, is zero. If the map has an invariant measure, which we assume, the theorem then states that the exponents larger than zero are well defined and form a discrete set, as in the continuous case [14], and since the norm of an operator is never smaller than its measure of non-compactness, the maximal exponent cannot be negative. The theorem gives no information below zero.

The two directions of the tangent space have a different meaning. A vector with $\delta\eta_0 = 1$ and $\delta z_{-1} = 0$ is a perturbation of the initial condition, and its observable is the derivative $\partial x_n/\partial x_0$, whose growth rate

$$\lambda_0(n) = \frac{1}{n} \ln \left| \frac{\partial x_n}{\partial x_0} \right| \tag{9}$$

is the quantity estimated by the Jacobian algorithm of Wu and Baleanu [10]. We call it the sensitivity to the initial condition. A vector with $\delta\eta_0 = 0$ is a perturbation of the memory alone, and the subspace $\{\delta\eta = 0\}$ is invariant. We compute the maximal exponent in this subspace, because a vector with $\delta\eta \neq 0$ keeps a constant component and its norm cannot decrease, whatever the dynamics. We use the algorithm of Benettin et al. [20]: a tangent vector is propagated with Eq. (8), it is renormalized when its norm becomes too large or too small, and the finite-time exponent between the ages n_0 and n is

$$\lambda(n_0, n) = \frac{1}{n - n_0} \ln \frac{\|v_n\|}{\|v_{n_0}\|}, \tag{10}$$

where n_0 is the age at which the tangent vector is initialized and the norm is defined in Section 2.4. When we need to follow the dependence on the age, we use the local expansion rate, defined by the same expression over an interval $[n_1, n_2]$ of ages, and we attribute it to the geometric mean age $\sqrt{n_1 n_2}$. To compute two exponents, as we do in Section 4.4, we propagate two tangent vectors and orthonormalize them at every step.

2.4. Quadrature of the modes

To compute the integrals in Eq. (5) we use the rate $s = -\ln r$ and its logarithm $u = \ln s$ as integration variables. Writing $d\beta = w(s)\, ds$, where w is

the density of β with respect to the rate, Eq. (3) becomes

$$c(m) = \int_{-\infty}^{\infty} e^{-me^u}\, w(e^u)\, e^u\, du, \tag{11}$$

with $w_{\mathrm{D}}(s) = \pi^{-1}\sin(\pi\nu)\, e^{-\nu s}(1-e^{-s})^{-\nu}$ and $w_{\mathrm{P}}(s) = \pi^{-1}\sin(\pi\nu)\, s^{-\nu}e^{-s}$. In the variable u the integrand is analytic in a strip around the real axis, it decays as $e^{(1-\nu)u}$ for $u \to -\infty$ and faster than exponentially for $u \to \infty$. For integrands of this kind the trapezoidal rule converges exponentially fast as the step decreases [21]. We therefore restrict the rate to an interval $[s_{\min}, s_{\max}]$, divide the interval $[\ln s_{\min}, \ln s_{\max}]$ into $M-1$ steps of width $h = 0.5$, and use the nodes $u_j = \ln s_{\min} + jh$, $j = 0, \ldots, M-1$, the decay factors $r_j = \exp(-e^{u_j})$ and the weights $W_j = h\, e^{u_j} w(e^{u_j})$. The map is then approximated by

$$z_n^{(j)} = r_j\, z_{n-1}^{(j)} + G_K(x_n), \qquad x_{n+1} = x_0 - \sum_{j=0}^{M-1} W_j\, z_n^{(j)}, \tag{12}$$

where $z_n^{(j)}$ is the value of the memory at the node r_j. The upper limit is $s_{\max} = 40/\nu$ for the FDLM and $s_{\max} = 40$ for the FLM, where the integrand is smaller than e^{-40} for every lag. The lower limit depends on the length N of the orbit. The modes with $s < s_{\min}$ carry a weight of the order of $s_{\min}^{1-\nu}$, while the kernel at the largest lag is of the order of $N^{\nu-1}$, and the ratio of the two is smaller than a prescribed tolerance ε if $s_{\min} = \varepsilon^{1/(1-\nu)}/N$. We use $\varepsilon = 10^{-10}$, so that the number of modes, $M \simeq 1 + [\ln s_{\max} - \ln s_{\min}]/h$, grows only as $\ln N/h$, and the accuracy is limited by the step h rather than by the truncation. The approximation (12) is a sum of exponentials for the kernel, of the type used for the fast evaluation of fractional integrals [22, 23, 24]; in discrete time it follows directly from the moment representation and requires no separate fitting step. Each step costs $O(M)$ operations, so that an orbit of length N costs $O(MN)$ operations instead of $O(N^2)$. The tangent map is discretized in the same way, and as norm of a tangent vector in the subspace $\{\delta\eta = 0\}$ we use $\|v\|^2 = \delta x^2 + \sum_j W_j (\delta z^{(j)})^2$. The term δx^2 is bounded by a multiple of the second one, so that the two norms are equivalent and give the same exponents.

3. The initial condition as a decaying forcing

The constant $\eta = x_0$ in Eq. (6) is never forgotten, and it is not obvious how it acts on the dynamics at large ages. To understand this point we invert

the convolution in Eq. (1), so as to express $G_K(x_n)$ in terms of the orbit, and we measure the orbit from a constant ξ, which for the moment is arbitrary. Let ζ be a formal variable and $C(\zeta) = \sum_{m\geq 0} c(m)\zeta^m$ the generating function of the kernel. We call $\hat{g}_m$ the coefficients of its reciprocal,

$$\sum_{m\geq 0} \hat{g}_m \zeta^m = \frac{1}{C(\zeta)}, \tag{13}$$

and $\psi(n) = \sum_{m=0}^{n} \hat{g}_m$ their partial sums. For the FDLM the generating function is $C(\zeta) = (1-\zeta)^{-\nu}$, so that the coefficients $\hat{g}_m$ are those of $(1-\zeta)^{\nu}$. They are the weights $\hat{g}_m = \Gamma(m-\nu)/[\Gamma(-\nu)\Gamma(m+1)]$ of the Grünwald–Letnikov approximation of the fractional derivative of order ν, which behave as $\hat{g}_m \simeq m^{-1-\nu}/\Gamma(-\nu)$ for large m, and their partial sums are $\psi(n) = \Gamma(n+1-\nu)/[\Gamma(1-\nu)\Gamma(n+1)]$. We also need the notion of a log-convex sequence, i.e., a positive sequence such that $c(m)^2 \leq c(m-1)\,c(m+1)$ for $m \geq 1$.

Proposition 2. *For every orbit of the map (1) and every constant ξ,*

$$G_K(x_n) = -\sum_{m=0}^{n} \hat{g}_m \left(x_{n+1-m} - \xi\right) + \left(x_0 - \xi\right)\psi(n), \qquad n \geq 0. \tag{14}$$

If the kernel is log-convex and $c(m) \simeq m^{\nu-1}/\Gamma(\nu)$ for large m, as is the case for both kernels (2), then $\hat{g}_m \leq 0$ for $m \geq 1$, the sequence $\psi(n)$ is positive and non-increasing, and

$$\psi(n) \simeq \frac{n^{-\nu}}{\Gamma(1-\nu)} \qquad (n \to \infty). \tag{15}$$

Before proving it, in the Appendix, let us see what the two terms of Eq. (14) mean. The first term is a fractional difference of order ν of the deviations $x_k - \xi$, computed with the memory starting at $k = 1$; it involves only the states $x_1, \ldots, x_{n+1}$ and does not contain x_0. The second term is a forcing that decays as $n^{-\nu}$ and is proportional to $x_0 - \xi$. For the FDLM the identity is the discrete counterpart of the relation $D^{\nu}_{\mathrm{RL}} x(t) = D^{\nu}_{\mathrm{C}} x(t) + x(0)\, t^{-\nu}/\Gamma(1-\nu)$ between the derivatives of order ν of Riemann–Liouville and of Caputo, both with lower terminal $t = 0$ [2], and it can also be obtained from the relation between the Riemann and Caputo fractional differences given by Abdeljawad [4]. The general form for log-convex kernels, and the interpretation that follows, are new to our knowledge.

The meaning of Eq. (14) becomes clear if we imagine that the orbit had a past. Consider the recurrence $G_K(x_n) = -\sum_{m\geq 0} \hat{g}_m x_{n+1-m}$, which is Eq. (14) with a memory extending to $-\infty$, and suppose that all the past states x_k with $k \leq 0$ are equal to x_0. Since $\sum_{m\geq 0} \hat{g}_m = \lim_n \psi(n) = 0$, we can subtract ξ from all the states without changing the sum, and the terms with $m > n$, which contain the past, contribute to the right-hand side the quantity $-(x_0 - \xi) \sum_{m>n} \hat{g}_m = (x_0 - \xi)\, \psi(n)$. This is exactly the forcing in Eq. (14). The Caputo map is therefore the recurrence with infinite memory in which the past has been frozen at the value x_0.

A typical past of a chaotic orbit would instead fluctuate around the time average of x. From now on we denote by $\bar{x}$ the average of x_n over a long orbit, which we assume not to depend on x_0, and we choose $\xi = \bar{x}$. With this choice, the difference between the frozen past and a typical past has two parts. The first is systematic, and it gives the forcing $(x_0 - \bar{x})\, \psi(n)$. The second is the sum of the fluctuations of a typical past weighted by the coefficients $\hat{g}_m$; for the FDLM, where $\hat{g}_m \sim m^{-1-\nu}$, it is of the order of $n^{-1/2-\nu}$ if the fluctuations are weakly correlated. The forcing is therefore the leading effect of the initial condition at large ages, and it vanishes when $x_0 = \bar{x}$.

Three predictions follow, and the next section is devoted to checking them. The first concerns orbits attracted by fixed points or periodic sinks, which we call regular orbits. Two orbits of the same map started from x_0 and x_0' differ by the forcing $(x_0 - x_0')\, \psi(n)$, which decays as $n^{-\nu}$. If the orbit follows this slowly vanishing forcing, its distance from the sink should decay in the same way, so that $\partial x_n / \partial x_0 \propto n^{-\nu}$ and $\lambda_0(n) \simeq -\nu \ln n / n$, which tends to zero. The second concerns chaotic orbits. If the statistics of the orbit respond linearly to a slowly varying forcing, i.e., if they change in proportion to its instantaneous amplitude, as in the linear response theory of chaotic systems [25], then an average computed over an interval of ages around n differs from its stationary value by a quantity proportional to $(x_0 - \bar{x})\, n^{-\nu}$. This applies in particular to the local expansion rate, with a coefficient whose sign is not known a priori. The third is that orbits started from $x_0 = \bar{x}$ should give stationary statistics from the beginning. The second prediction is the discrete form of the conjecture of [14] on the convergence of the finite-time exponents of fractional-order systems, in which the origin and the scaling of the memory term are now identified.

4. Numerical results

4.1. Accuracy and cost

Figure 1(a) shows the relative error of the quadrature (12) on the kernels (2), for $\nu = 0.3$, 0.5 and 0.7 and for all lags up to $m = 10^8$, with the nodes chosen for $N = 10^8$. The error is below $4 \cdot 10^{-7}$ for the FDLM and below $2 \cdot 10^{-8}$ for the FLM, with M between 112 and 114 modes at $\nu = 0.3$ and between 199 and 200 at $\nu = 0.7$. When the dynamics is regular, the orbits computed with Eq. (12) coincide within 10^{-7} with those computed with the full sum (1) over $2 \cdot 10^4$ steps. In the chaotic regime two such orbits separate after a few tens of steps, as any two numerical orbits of a chaotic map do, and the comparison has to be made on statistics. For the FDLM at $\nu = 0.3$ and $K = 3.2$, over $4 \cdot 10^4$ steps, the average of x is 0.5659 with the full sum and 0.5662 with the modes, the standard deviations are 0.2562 and 0.2560, and the finite-time exponents are 0.350 and 0.344, a difference compatible with the fluctuations of an exponent over such a short orbit. The method also reproduces the thresholds of the first bifurcation at $\nu = 0.5$ reported by Edelman [8], $K = 1 + \sqrt{2} \simeq 2.414$ for the FDLM and $K \simeq 3.930$ for the FLM: with orbits of $2 \cdot 10^5$ steps we find the fixed point stable at $K = 2.41$ and 3.92, respectively, and a period-two orbit at $K = 2.42$ and 3.94.

The gain in time is shown in Fig. 1(b), measured on a single core of a server. With the full sum an orbit of $4 \cdot 10^4$ steps costs 0.64 s, and since the cost grows as N^2 an orbit of 10^8 steps would require about $4 \cdot 10^6$ s, i.e., more than a month. With the modes an orbit of 10^7 steps costs 2.7 s, and the same orbit of 10^8 steps requires less than a minute. On the ten cores of the laptop used for the runs of Section 4.3, a set of 150 orbits of 10^8 steps with their tangent vectors takes six to seven minutes.

4.2. Chaos at low orders and zero exponents

Figure 2 shows the bifurcation diagrams and the maximal exponent of the two maps at $\nu = 0.3$. For each value of K we start the orbit from $x_0 = 0.3$ for the FDLM and from $x_0 = 0.001$ for the FLM, as in [8], follow it for $6 \cdot 10^4$ steps, plot the last 200 values and compute the exponent with Eq. (10) from $n_0 = 2 \cdot 10^4$. Both maps go through a cascade of period doublings followed by chaos, interrupted by periodic windows. Taking as chaotic the values of K at which the exponent exceeds 10^{-2}, the FDLM is chaotic for $3.06 \lesssim K \lesssim 3.44$ and the FLM for $7.79 \lesssim K \lesssim 8.94$; for larger K the orbits escape to infinity, and for the FLM the scan ends at $K = 8.95$, the first value at which this

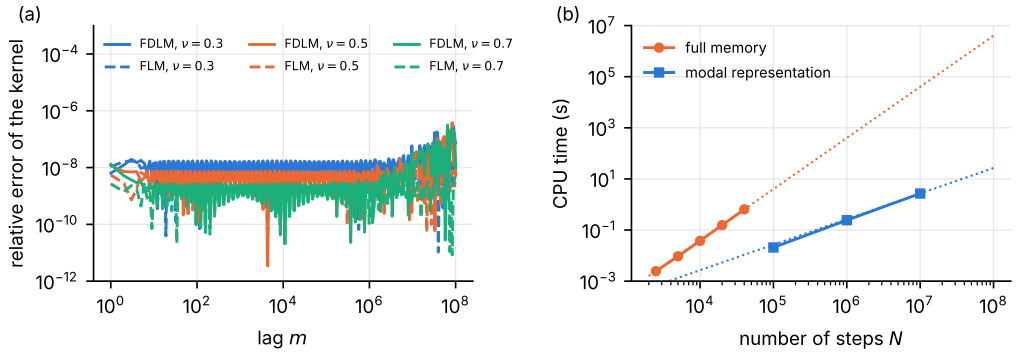

Figure 1: (a) Relative error of the quadrature (12) on the kernels of the FDLM (solid lines) and of the FLM (dashed lines) for $\nu = 0.3$, 0.5 and 0.7, as a function of the lag m, with step $h = 0.5$ and nodes chosen for orbits of 10^8 steps. (b) Computing time on a single core for an orbit of the FDLM with $\nu = 0.3$ and $K = 3.2$, with the full sum (1) (circles) and with the representation on modes (squares). The dotted lines are the extrapolations proportional to N^2 and N.

happens. The maximal exponent reaches 0.45 and 0.48, respectively. Similar scans at $\nu = 0.2$, 0.35, 0.4 and 0.5, not shown, give the same sequence of period doublings and chaos. In the regular regimes the computed exponent is never smaller than $-5 \cdot 10^{-6}$ at $n = 6 \cdot 10^4$: perturbations of the memory neither grow nor contract exponentially, and the exponent is zero within the resolution of a finite orbit.

The exponent of Fig. 2 concerns perturbations of the memory. The other direction of the tangent space, the perturbation of the initial condition, is shown in Fig. 3, which reports the envelope of $|\partial x_n/\partial x_0|$ along regular orbits of the FDLM at three orders. The derivative decays as $n^{-\nu}$ from $n \simeq 10^2$ to $n = 10^6$. Fitting a power law to the envelope for $10^4 \leq n \leq 10^6$ we find the exponents 0.30 and 0.31 at $\nu = 0.3$ (with $K = 2.2$, where the attractor is a fixed point and which is not shown in the figure, and with $K = 2.8$, where it is a period-two orbit), 0.50 at $\nu = 0.5$ and 0.70 at $\nu = 0.7$; for the FLM at $\nu = 0.3$ and $K = 6.5$, not shown in the figure, we find 0.31. This is the decay of the forcing in Proposition 2: the regular orbit simply follows the slowly vanishing memory of its starting point. The sensitivity (9) therefore behaves as $\lambda_0(n) \simeq -\nu \ln n/n + A/n$, where A is the logarithm of the prefactor of the decay. Its measured value after 10^3 iterations is between -0.0025 for $\nu = 0.3$ and -0.006 for $\nu = 0.7$, and after 10^6 iterations it is of the order of -10^{-5}. Negative estimates of this size are thus to be expected from computations

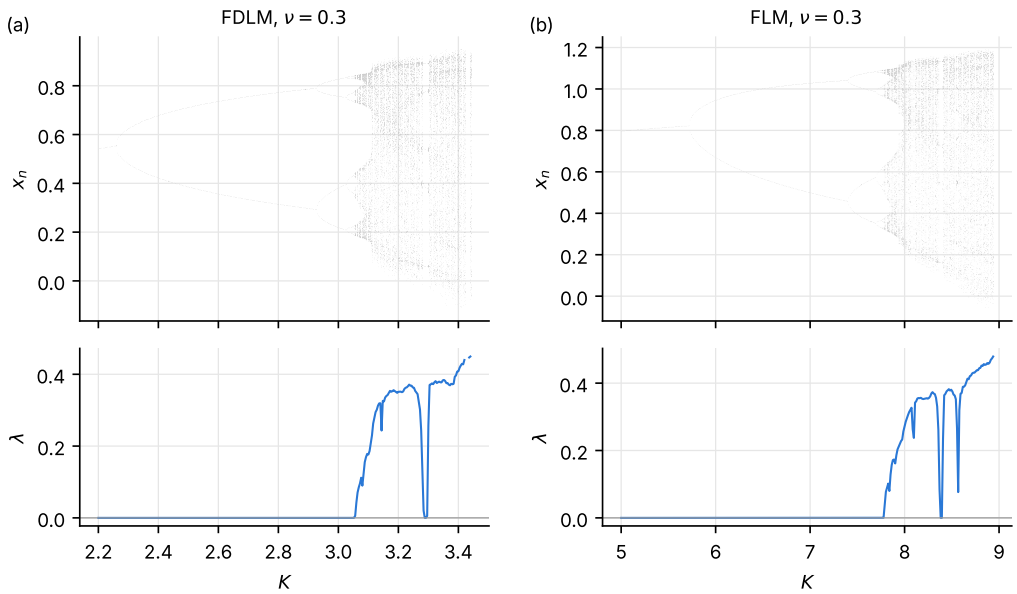

Figure 2: Bifurcation diagrams (top) and maximal Lyapunov exponent (bottom) of the FDLM (a) and of the FLM (b) at $\nu = 0.3$. For each K the orbit has length $6 \cdot 10^4$, the last 200 values are shown, and the exponent is computed in the subspace $\{\delta\eta = 0\}$ from the age $2 \cdot 10^4$.

over short horizons, while the limit is zero. Since neither direction grows, the maximal exponent of a regular orbit is zero, and not only non-negative.

4.3. Ageing of chaotic statistics

To see the effect of the initial condition in the chaotic regime we compare orbits of the FDLM with the same parameters and different initial conditions. For each initial condition we follow 50 orbits, obtained by adding to x_0 perturbations not larger than $5 \cdot 10^{-8}$, which make the orbits independent after a few tens of steps. The tangent vector is initialized at the age $n_0 = 10^3$ in a random direction of the subspace $\{\delta\eta = 0\}$. The local expansion rate and the average of x are computed over intervals of ages whose ends, measured from n_0, grow geometrically by a factor of about five for the orbits of 10^8 steps and of about four for those of 10^7 steps. For each statistic we denote by Δ the difference between its mean over the orbits started from a given x_0 and its mean over a set of reference orbits started close to $\bar{x}$, and by p the exponent of the decay $|\Delta| \propto n^{-p}$. The reference values were chosen from

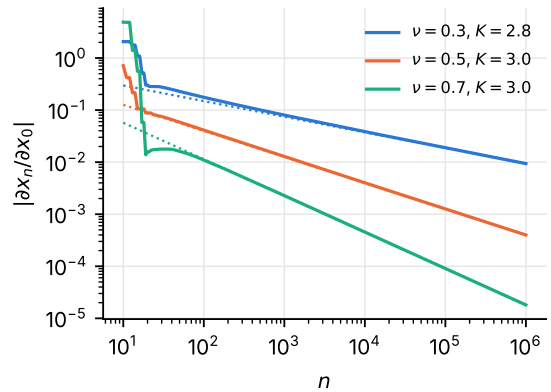

Figure 3: Envelope of the derivative of the observable with respect to the initial condition along regular orbits of the FDLM, for $\nu = 0.3$ ($K = 2.8$), $\nu = 0.5$ ($K = 3.0$) and $\nu = 0.7$ ($K = 3.0$), with $x_0 = 0.3$. The dotted lines are proportional to $n^{-\nu}$.

rough preliminary estimates of $\bar{x}$, while the values of $\bar{x}$ reported below come from orbits of 10^7 steps. At $\nu = 0.3$ and $\nu = 0.35$, with $K = 3.2$, we use $x_0 = 0.25$ and 0.40, the reference $x_0 = 0.56$ and orbits of 10^8 steps. At $\nu = 0.4$ ($K = 3.3$) and $\nu = 0.5$ ($K = 3.35$) we use $x_0 = 0.25$, the reference $x_0 = 0.55$ and orbits of 10^7 steps. The standard errors quoted below are those of the means over the orbits of each set. To judge their size it is useful to recall that the autocorrelation of x_n along a chaotic orbit at $\nu = 0.3$ falls below 0.05 in five steps.

Figure 4(a) shows the local expansion rate at $\nu = 0.3$ as a function of the age. Here $\bar{x} = 0.5611$, and the reference orbits are stationary from the beginning: their expansion rate, which we take as the stationary maximal exponent λ_1, is $\lambda_1 = 0.3626$ within 10^{-3} from the first interval of ages, around $1.5 \cdot 10^3$, and within $2 \cdot 10^{-4}$ from the age 10^4 to the age $4.4 \cdot 10^7$, while the average of x does not change in the fourth decimal place. The orbits started from $x_0 = 0.25$ and 0.40 have instead, at the age $1.3 \cdot 10^4$, an expansion rate smaller by 0.010 and 0.013, and they approach λ_1 very slowly: at the age $4.4 \cdot 10^7$ the deficits are still $2.34 \cdot 10^{-3}$ and $1.08 \cdot 10^{-3}$, with standard errors of 10^{-5}. The memory of the initial condition thus survives for a time seven orders of magnitude longer than the correlation time, and it is resolved well above the statistical errors. At intermediate ages the two deficits are not ordered as the distances from $\bar{x}$, but from the age 10^5 onwards the larger deficit belongs to the orbits started farther from $\bar{x}$. As shown in Fig. 4(b), at

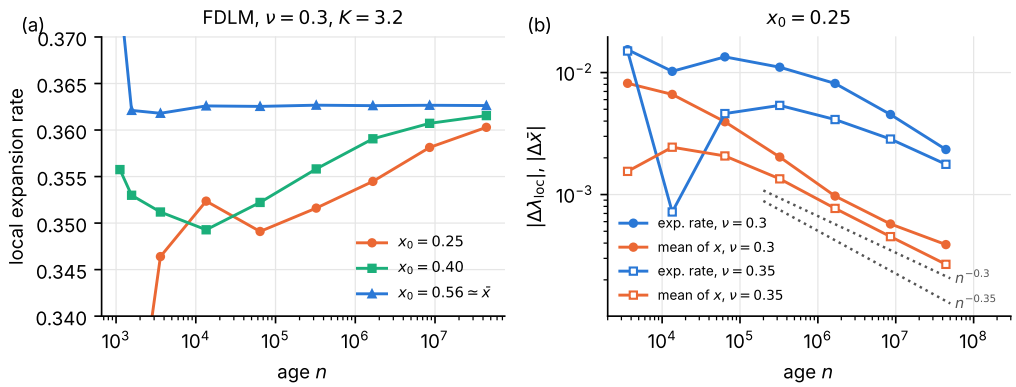

Figure 4: Ageing of the chaotic statistics of the FDLM with $K = 3.2$. (a) Local expansion rate at $\nu = 0.3$ as a function of the age, for orbits started from $x_0 = 0.25$ (circles), 0.40 (squares) and $0.56 \simeq \bar{x}$ (triangles), averaged over 50 orbits. (b) Absolute differences of the local expansion rate (blue) and of the average of x (orange) between the orbits started from $x_0 = 0.25$ and those started from $x_0 = 0.56$, at $\nu = 0.3$ (filled symbols) and $\nu = 0.35$ (open symbols). The dotted lines are proportional to $n^{-\nu}$.

large ages the differences decay as a power of the age, both for the expansion rate and for the average of x. At $\nu = 0.35$ the difference of the expansion rate changes sign near the age $1.5 \cdot 10^4$, which appears in the figure as a dip of its absolute value, and decays as a power only after the age 10^5.

Table 1 reports the exponents p obtained by fitting a straight line to $\ln|\Delta|$ as a function of $\ln n$ over the last four intervals of ages, which extend from $3 \cdot 10^5$ to $4.4 \cdot 10^7$ for the orbits of 10^8 steps and from $7 \cdot 10^4$ to $5 \cdot 10^6$ for those of 10^7 steps. The exponents are close to ν: between 0.26 and 0.38 at $\nu = 0.3$, between 0.23 and 0.33 at $\nu = 0.35$, 0.35 at $\nu = 0.4$ and between 0.46 and 0.48 at $\nu = 0.5$. They are not yet converged, however. The local slopes of $\ln|\Delta|$ between consecutive intervals still change at the largest ages: at $\nu = 0.35$ the slope for the average of x is stable between 0.31 and 0.34 over the last three intervals, while the slope for the expansion rate grows from 0.16 to 0.29 for $x_0 = 0.25$. The fitted values also depend on the length of the orbits: at $\nu = 0.3$ and $x_0 = 0.25$ a set of orbits of 10^7 steps, with reference $x_0 = 0.55$, gives $p \simeq 0.2$ for the expansion rate instead of the value 0.32 obtained with orbits of 10^8 steps. Taken together, these numbers tell us that at large ages the decay is algebraic with an exponent close to ν, as predicted in Section 3, but they do not determine the exponent with a precision better than about 0.1.

Table 1: Ageing of chaotic statistics in the FDLM. For each order ν and parameter K: time average $\bar{x}$ of the observable, maximal exponent λ_1 of the reference orbits at the largest age, and exponent p of the decay $|\Delta| \propto n^{-p}$ of the differences of the local expansion rate and of the average of x between the orbits started from x_0 and the reference orbits, started from $x_0 = 0.56$ ($\nu = 0.3$, 0.35) or 0.55 ($\nu = 0.4$, 0.5).

ν	K	$\bar{x}$	λ_1	x_0	p (exp. rate)	p (mean of x)	orbits
0.30	3.20	0.5611	0.3626	0.25	0.32	0.34	3×50, 10^8
				0.40	0.38	0.26	
0.35	3.20	0.5731	0.3473	0.25	0.23	0.33	3×50, 10^8
				0.40	0.28	0.31	
0.40	3.30	0.5642	0.3272	0.25	0.35	0.35	2×50, 10^7
0.50	3.35	0.5806	0.3555	0.25	0.46	0.48	2×50, 10^7

The amplitude of the effect is, at the largest ages, roughly proportional to the distance of x_0 from the reference. At $\nu = 0.3$ the ratio of the differences produced by $x_0 = 0.25$ and by $x_0 = 0.40$ at the age $4.4 \cdot 10^7$ is 2.2 for the expansion rate and 1.8 for the average of x, and at $\nu = 0.35$ it is 1.8 for both, to be compared with $(0.56 - 0.25)/(0.56 - 0.40) = 1.9$. The sign of the effect, on the other hand, depends on the order. At $\nu = 0.3$ the orbits started below $\bar{x}$ have a smaller expansion rate than the reference orbits, while at $\nu = 0.4$ and 0.5 they have a larger one.

The choice of the reference deserves a comment. At $\nu = 0.35$ we used the value $x_0 = 0.56$, estimated at $\nu = 0.3$, and it turned out to be about 0.013 below the time average $\bar{x} = 0.5731$. The reference orbits are then not stationary: their expansion rate decreases from 0.3491 at the age $3.6 \cdot 10^3$ to 0.3473 at the age $4.4 \cdot 10^7$, and the average of x decreases by $2.6 \cdot 10^{-4}$. A linear scaling of the effect observed for $x_0 = 0.25$, which is twenty-five times farther from $\bar{x}$, would predict an increase of the expansion rate of about $7 \cdot 10^{-4}$. The drift is thus not explained by the linear picture, and since it is of the same order as the differences used in the fit, the exponents of the expansion rate at $\nu = 0.35$ in Table 1 are less reliable than the others. The same caution applies at $\nu = 0.4$, where the expansion rate of the reference orbits, started 0.014 from $\bar{x}$, decreases from 0.3315 to 0.3272. At $\nu = 0.5$, where the effect decays faster, the reference orbits started 0.03 from $\bar{x}$ have an expansion rate constant within $4 \cdot 10^{-4}$ from the age $5 \cdot 10^3$. The accuracy with which $\bar{x}$ must be known therefore depends on the order: at $\nu = 0.3$ and 0.35 an error of 10^{-3} is harmless and one of 10^{-2} is not.

At $\nu = 0.2$, finally, the dependence on the initial condition is much stronger. With $K = 3.3$, orbits started from different values of x_0 have expansion rates that still differ by about ten per cent at the age $4 \cdot 10^5$, and in this case we could not identify the scaling observed at the larger orders.

4.4. A two-dimensional map

To check that these results do not depend on the logistic nonlinearity we consider a fractional version of the Hénon map, written in the same form as Eq. (1); fractional maps of Hénon type have been studied, for instance, in [9]. The state is now the vector $\mathbf{x}_n = (x_n, y_n)$, both components have the kernel c_{D}, and the map is

$$\mathbf{x}_{n+1} = \mathbf{x}_0 - \sum_{k=0}^{n} c_{\mathrm{D}}(n-k)\, \mathbf{G}(\mathbf{x}_k), \qquad \mathbf{G}(x,y) = \Big(x - 1 + ax^2 - y,\ y - bx\Big), \tag{16}$$

where a and b are the parameters of the Hénon map, to which Eq. (16) reduces for $\nu = 1$: $x_{n+1} = 1 - ax_n^2 + y_n$, $y_{n+1} = bx_n$. Each component has its own memory, so that the number of modes is doubled, and Proposition 2 holds for each component, with the forcing $(\mathbf{x}_0 - \bar{\mathbf{x}})\, \psi(n)$, where $\bar{\mathbf{x}} = (\bar{x}, \bar{y})$ is the time average of the orbit. With the classical value $b = 0.3$ we found chaos only in a narrow interval of a at $\nu = 0.5$ and none at $\nu \leq 0.4$, so we lowered b to 0.1. With the same criterion used for the logistic maps, the map is then chaotic, with periodic windows, for $0.61 \lesssim a \lesssim 0.94$ at $\nu = 0.4$ and for $0.51 \lesssim a \lesssim 0.79$ at $\nu = 0.3$, and the orbits escape to infinity for larger values of a. We also computed the second exponent λ_2, with two tangent vectors in the subspace $\{\delta\eta = 0\}$ orthonormalized at every step with the norm of Section 2.4. In all the chaotic runs λ_2 is zero within 10^{-7}, whereas the Hénon map has a negative second exponent. This agrees with the conjecture of [14] that fractional systems have no negative exponents, but it is not an independent test, since the algorithm cannot resolve exponents below the essential exponent, which is zero.

For the ageing test we fixed $b = 0.1$ and took $a = 0.75$ at $\nu = 0.4$ and $a = 0.55$ at $\nu = 0.3$. For each order we followed 30 orbits of 10^7 steps for each of three initial conditions, which differ only in x_0, while y_0 is set close to $\bar{y}$. At $\nu = 0.4$ the time averages are $\bar{x} = 0.1289$ and $\bar{y} = 0.0129$, and we used $y_0 = 0.013$ and $x_0 = -0.4$, -0.1 and 0.129, the last one as reference. At $\nu = 0.3$ they are $\bar{x} = -0.1081$ and $\bar{y} = -0.0107$, and we used $y_0 = -0.011$ and $x_0 = 0.4$, 0.15 and -0.109. The results, shown in Fig. 5, reproduce those

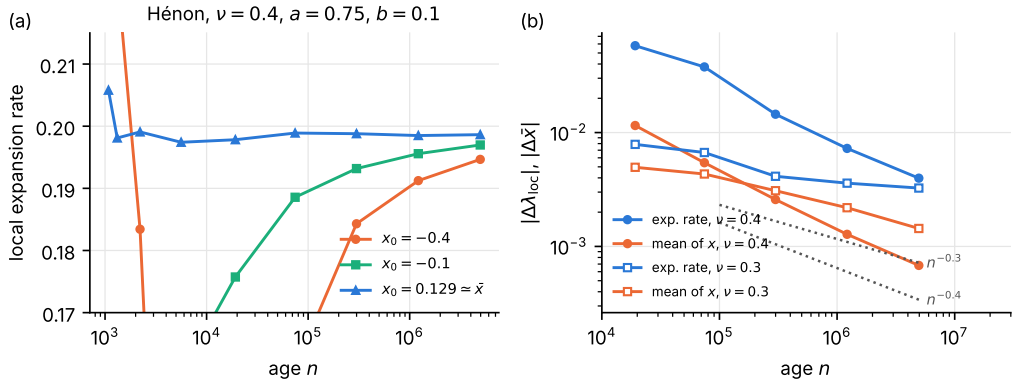

Figure 5: Ageing of the chaotic statistics of the fractional Hénon map (16) with $b = 0.1$. (a) Local expansion rate at $\nu = 0.4$ and $a = 0.75$ as a function of the age, for orbits started from $x_0 = -0.4$ (circles), -0.1 (squares) and $0.129 \simeq \bar{x}$ (triangles), averaged over 30 orbits. The values of the orbits started from $x_0 = -0.4$ at ages below 10^4 are outside the plotted range. (b) Absolute differences of the local expansion rate (blue) and of the average of x (orange) between the orbits started farthest from $\bar{x}$ and the reference orbits, at $\nu = 0.4$ (filled symbols, $a = 0.75$) and $\nu = 0.3$ (open symbols, $a = 0.55$). The dotted lines are proportional to $n^{-\nu}$.

of the logistic map. The reference orbits are stationary from the beginning: at $\nu = 0.4$ their expansion rate is $\lambda_1 = 0.1986$ within $4 \cdot 10^{-4}$ from the age $2 \cdot 10^4$, and at $\nu = 0.3$ it is $\lambda_1 = 0.1569$ within 10^{-3} from the age $1.3 \cdot 10^3$. The orbits started far from $\bar{x}$ show a deficit of the expansion rate which, for $x_0 = -0.4$ at $\nu = 0.4$, is still $4 \cdot 10^{-3}$ at the age $5 \cdot 10^6$, with a standard error of $4 \cdot 10^{-5}$. At $\nu = 0.4$ the differences of the expansion rate and of the average of x decay with exponents between 0.43 and 0.53 over the last four intervals and with local slopes between 0.40 and 0.45 over the last two, close to ν. Their amplitudes are proportional to the distance from the reference: the ratio of the differences produced by $x_0 = -0.4$ and by $x_0 = -0.1$ at the largest age is 2.4 for both quantities, against $(0.129 + 0.4)/(0.129 + 0.1) = 2.3$. At $\nu = 0.3$ the differences of the average of x decay with local slopes between 0.24 and 0.37, again close to ν, and the ratio of their amplitudes is 2.1, against $(0.4 + 0.109)/(0.15 + 0.109) = 2.0$. The differences of the expansion rate decay more slowly, with exponents between 0.1 and 0.2, as we found for the logistic map with orbits of the same length.

5. Discussion

With the representation on memory modes a fractional map becomes a dynamical system in the usual sense. Its state contains all the information needed to continue the orbit, and the tangent map acts on the same state, so that the Lyapunov exponents are those of an autonomous map. In particular, we never need to choose a length at which the memory is truncated, a choice that affects many computations of exponents of fractional systems [12, 13, 14]. The structure of the tangent map, a contraction with spectrum $[0, 1]$ plus an operator of rank one, prevents the maximal exponent from being negative, and the data show that along regular orbits it is in fact zero: perturbations of the memory do not grow, and the derivative with respect to the initial condition decays as $n^{-\nu}$, with the exponent of the forcing of Proposition 2. The negative values reported for fractional maps in regular regimes, noted by Edelman [7], may be finite-time estimates of this kind, whose size after 10^3 iterations is a few thousandths; a direct comparison with the published values would require the same horizons and initial conditions. There is also a practical gain, since the cost linear in the length of the orbit makes the long transients of these maps at low orders easy to follow.

The main result concerns the chaotic regime. The initial condition acts as a forcing that decays as a power of the age, and this forcing produces a slow drift of all the statistics, including the local expansion rate, which at $\nu = 0.3$ and 0.35 is still visible after 10^7 iterations. As a consequence, a Lyapunov exponent computed along an orbit of finite length depends both on the initial condition and on the length of the orbit. This recalls the dependence of the bifurcation diagrams on the same two quantities observed by Edelman [8], although that dependence concerns the selection of attractors and the transients of regular orbits rather than the drift of chaotic statistics. The drift can be reduced to the level of the statistical errors by starting the orbit close to the time average of x, which can be estimated with a preliminary run: at $\nu = 0.3$, an orbit started about 10^{-3} from $\bar{x}$ gives a stationary expansion rate from the first interval of ages that we measure. When this is not possible, the age of the orbit should be reported together with the exponent. One might also think of averaging over random initial conditions. Since the effect is roughly linear in $x_0 - \bar{x}$, this cancels the leading term only if the initial conditions are distributed around $\bar{x}$, which requires the same knowledge of $\bar{x}$ as the choice $x_0 \simeq \bar{x}$.

Our original motivation was the continuous case, and here the discrete

maps give us what the fractional oscillators could not. For fractional-order differential systems we conjectured in [14] that the finite-time exponents converge with a memory term proportional to $t^{-\nu}$, which can be observed only for $\nu < 1/2$. The discrete maps make this regime accessible, and the decay that we observe is algebraic with exponents close to ν, between 0.23 and 0.38 for $\nu = 0.3$ and 0.35, and between 0.35 and 0.48 for $\nu = 0.4$ and 0.5. Proposition 2 identifies the origin of the term and its scaling, $(x_0 - \bar{x})\, n^{-\nu}/\Gamma(1-\nu)$, while the response coefficient of each statistic, including its sign, remains unknown. The residual differences between the measured exponents and ν may be due to the slow approach to the asymptotic regime, to the next corrections, of the order of $n^{-1/2-\nu}$ if the fluctuations are weakly correlated, or to the long-range correlations of the slow modes, whose variance in a stationary orbit is not bounded for $\nu \leq 1/2$ [14]. This last effect would also make the estimate $n^{-1/2-\nu}$ of the fluctuating part optimistic at low orders. Our data do not allow us to separate these contributions.

We have left several questions open, and it is fair to list them. The existence of a stationary dynamics on the space of modes, and of an invariant measure with respect to which the exponents are defined, is assumed and not proved, as in the continuous case. The predictions of Section 3 rely on a linear response of the statistics to a slowly decaying forcing, which is plausible but not proved for maps with memory, and the drift of the reference orbits at $\nu = 0.35$ shows that it is at best approximate. The numerical study of ageing is limited to the falling-factorial kernel and to the logistic and Hénon nonlinearities, and at $\nu = 0.2$ we could not identify a scaling law. The method, on the other hand, applies without changes to maps of any dimension and to any kernel that is a moment sequence, for instance kernels with tempered power-law decay or of distributed order: in all these cases only the measure in Eq. (3) changes, while the structure of the state space and of the tangent map remains the same.

6. Conclusions

The memory of a fractional map of Caputo type can be carried by one or two hundred geometric modes. This follows from the fact that its kernel is a moment sequence, and it turns the map into an autonomous dynamical system on which Lyapunov exponents can be defined without truncating the memory and computed at a cost linear in the length of the orbit. Once the map is written in this way, the initial condition stops being a mysterious ingredient

and becomes a forcing, proportional to $(x_0 - \bar{x})\, n^{-\nu}$, that we can see, measure and, if we wish, remove. Along regular orbits it makes the sensitivity to the initial condition decay as $n^{-\nu}$, so that the exponents are zero. Along chaotic orbits it makes the statistics, including the local expansion rate, depend on the initial condition for times far longer than the correlation time, with a decay whose exponent is close to ν; orbits started near the time average do not show this drift, and we suggest this choice, or the declaration of the age of the orbit, as a rule for the computation of exponents of fractional maps. The same behaviour is found in the FDLM and in a two-dimensional map of Hénon type. Edelman listed a consistent quantitative description of chaos in discrete fractional systems among the open problems of the field; we believe that the space of memory modes is the natural setting in which such a description can be built, and that the ageing it reveals is not a numerical nuisance but a property of dynamics with memory, which in discrete time becomes directly observable.

Appendix A. Proof of Proposition 2

Let $e_n = x_{n+1} - x_0$ and $\gamma_n = G_K(x_n)$ for $n \geq 0$, and let $C(\zeta) = \sum_{m\geq 0} c(m)\zeta^m$, $E(\zeta) = \sum_n e_n \zeta^n$ and $\Phi(\zeta) = \sum_n \gamma_n \zeta^n$ be their generating functions, considered as formal power series. Equation (1) states that e is the convolution of c and $-\gamma$, i.e., $E = -C\Phi$. Since $c(0) > 0$, the series C has a reciprocal $\hat{G}(\zeta) = \sum_m \hat{g}_m \zeta^m$, and $\Phi = -\hat{G}E$, that is, $\gamma_n = -\sum_{m=0}^{n} \hat{g}_m e_{n-m}$. Writing $e_{n-m} = (x_{n+1-m} - \xi) + (\xi - x_0)$ and using $\sum_{m=0}^{n} \hat{g}_m = \psi(n)$ we obtain Eq. (14).

Both kernels (2) are log-convex, since every moment sequence of a positive measure has this property by the Cauchy–Schwarz inequality, and both behave as $m^{\nu-1}/\Gamma(\nu)$ for large m. By a theorem of Kaluza [26], the reciprocal of the generating function of a positive log-convex sequence has coefficients $\hat{g}_m \leq 0$ for $m \geq 1$, and ψ is therefore non-increasing. To find its limit and its asymptotic behaviour we note that $\sum_n \psi(n)\zeta^n = \hat{G}(\zeta)/(1-\zeta) = 1/[(1-\zeta)C(\zeta)]$. Since $c(m) \simeq m^{\nu-1}/\Gamma(\nu)$, the Abelian theorem for power series gives $C(\zeta) \simeq (1-\zeta)^{-\nu}$ for $\zeta \to 1^-$ [27, Ch. XIII.5], and therefore $\sum_n \psi(n)\zeta^n \simeq (1-\zeta)^{\nu-1}$. Since $C(\zeta) \to \infty$, the limit of $\psi(n)$ is zero, and a non-increasing sequence that tends to zero is non-negative; it is in fact positive, because if ψ vanished at some n it would vanish from then on, contradicting the asymptotic behaviour found below. The Tauberian theorem of Hardy, Littlewood and Karamata, which applies to monotone sequences [27,

Ch. XIII.5], then gives $\psi(n) \simeq n^{-\nu}/\Gamma(1-\nu)$. For the FDLM the same result follows directly from the explicit expression of $\psi(n)$ and from the asymptotic behaviour of the ratio of gamma functions. $\square$

Data availability

The data and the Python code used for the computations are available from the author on reasonable request.

References

[1] C. Lubich, Discretized fractional calculus, SIAM Journal on Mathematical Analysis 17 (1986) 704–719.

[2] I. Podlubny, Fractional Differential Equations, Academic Press, San Diego, 1999.

[3] F.M. Atici, P.W. Eloe, Initial value problems in discrete fractional calculus, Proceedings of the American Mathematical Society 137 (2009) 981–989.

[4] T. Abdeljawad, On Riemann and Caputo fractional differences, Computers & Mathematics with Applications 62 (2011) 1602–1611.

[5] G.-C. Wu, D. Baleanu, Discrete fractional logistic map and its chaos, Nonlinear Dynamics 75 (2014) 283–287.

[6] M. Edelman, Stability of fixed points and chaos in fractional systems, arXiv:1711.06777 (2017).

[7] M. Edelman, Stability of fixed points in generalized fractional maps of the orders $0 < \alpha < 1$, arXiv:2209.01719 (2022).

[8] M. Edelman, On fractional generalizations of the logistic map and their applications, arXiv:2503.13256 (2025).

[9] A. Ouannas, A.-A. Khennaoui, X. Wang, V.-T. Pham, S. Boulaaras, S. Momani, Bifurcation and chaos in the fractional form of Hénon–Lozi type map, The European Physical Journal Special Topics 229 (2020) 2261–2273.

[10] G.-C. Wu, D. Baleanu, Jacobian matrix algorithm for Lyapunov exponents of the discrete fractional maps, Communications in Nonlinear Science and Numerical Simulation 22 (2015) 95–100.

[11] R. Caponetto, S. Fazzino, A semi-analytical method for the computation of the Lyapunov exponents of fractional-order systems, Communications in Nonlinear Science and Numerical Simulation 18 (2013) 22–27.

[12] M.-F. Danca, N. Kuznetsov, Matlab code for Lyapunov exponents of fractional-order systems, International Journal of Bifurcation and Chaos 28 (2018) 1850067.

[13] M.-F. Danca, M. Fečkan, Memory principle of the Matlab code for Lyapunov exponents of fractional order, arXiv:2406.04686 (2024).

[14] S. Fazzino, Lyapunov exponents of fractional-order systems: a definition from the diffusive representation, the ageing of memory, and what memory truncation measures, preprint, Research Square (2026), doi:10.21203/rs.3.rs-11383967/v1.

[15] G. Montseny, Diffusive representation of pseudo-differential time-operators, ESAIM: Proceedings 5 (1998) 159–175.

[16] D.V. Widder, The Laplace Transform, Princeton University Press, Princeton, 1941.

[17] R.A.C. Ferreira, On the complete monotonicity of the solutions to some Volterra difference equations, preprint, Centro de Matemática da Universidade do Porto (2026).

[18] D. Ruelle, Characteristic exponents and invariant manifolds in Hilbert space, Annals of Mathematics 115 (1982) 243–290.

[19] P. Thieullen, Fibrés dynamiques asymptotiquement compacts. Exposants de Lyapounov. Entropie. Dimension, Annales de l'Institut Henri Poincaré, Analyse Non Linéaire 4 (1987) 49–97.

[20] G. Benettin, L. Galgani, A. Giorgilli, J.-M. Strelcyn, Lyapunov characteristic exponents for smooth dynamical systems and for Hamiltonian systems; a method for computing all of them. Part 1: Theory, Meccanica 15 (1980) 9–20.

[21] L.N. Trefethen, J.A.C. Weideman, The exponentially convergent trapezoidal rule, SIAM Review 56 (2014) 385–458.

[22] G. Beylkin, L. Monzón, Approximation by exponential sums revisited, Applied and Computational Harmonic Analysis 28 (2010) 131–149.

[23] D. Baffet, J.S. Hesthaven, A kernel compression scheme for fractional differential equations, SIAM Journal on Numerical Analysis 55 (2017) 496–520.

[24] S. Jiang, J. Zhang, Q. Zhang, Z. Zhang, Fast evaluation of the Caputo fractional derivative and its applications to fractional diffusion equations, Communications in Computational Physics 21 (2017) 650–678.

[25] D. Ruelle, A review of linear response theory for general differentiable dynamical systems, Nonlinearity 22 (2009) 855–870.

[26] T. Kaluza, Über die Koeffizienten reziproker Potenzreihen, Mathematische Zeitschrift 28 (1928) 161–170.

[27] W. Feller, An Introduction to Probability Theory and Its Applications, Vol. II, 2nd ed., Wiley, New York, 1971.